ACS EARTH AND SPACE CHEMISTRY

http://pubs.acs.org/journal/aesccq

Article

Biodegradation of Polycyclic Aromatic Hydrocarbons: A Case Study of the Chepaizi Uplift, Junggar Basin, NW China

Xue Chen, Ningrui Yang, Xiao Jin, Ruihui Zheng, Yunpeng Zhang, and Zhihuan Zhang*

Cite This: *ACS Earth Space Chem.* 2023, 7, 823−837

Read Online

ACCESS | Metrics & More | Article Recommendations | Supporting Information

ABSTRACT: Polycyclic aromatic hydrocarbons (PAHs) are important components in crude oil with extensive applications in maturity assessment, depositional environment reconstruction, and oil−oil/source rock correlation. The biodegradation of oils is common under geological conditions. Despite many studies on the biodegradation of saturated hydrocarbons, naphthalenes, and phenanthrenes, the relative susceptibilities to biodegradation of fluorene, dibenzothiophene, chrysene, pyrene and their alkylated homologues, and triaromatic steroid hydrocarbons were not well studied. In this study, a suite of oils and oil sands from the Chepaizi Uplift, Junggar Basin, were collected to investigate the fate and relative susceptibilities to the biodegradation of these PAHs under geological conditions. Gas chromatography−mass spectrometry analysis was conducted to identify the aromatic species. Based on the studied samples with different biodegradation levels, the relative susceptibilities of individual dibenzothiophene, fluorene, chrysene, and pyrene and their alkylated homologues and triaromatic steroid hydrocarbons were determined. DBT/1-MDBT, 3,7-/2,4-DMDBT, 1,2,7-+1,2,8-/2,4,6-TMDBT, 1-MF/4-MF, 1,6-DMF/B, Py/4-MPy, and C_{26}20S TAS/C_{27}20R TAS were proposed to assess the biodegradation. The biodegradation order is not related to thermodynamic stability, making the maturity assessment of biodegraded oils and oil sands more difficult. Moreover, most PAH-based parameters used for oil−oil/source rock correlation and depositional environment analysis are not available due to biodegradation. Maturity parameters, such as MCI1, MCI2, and MChyI2, increase with increasing biodegradation, while MDR and DMDBTI decrease with increasing biodegradation. However, the refractory C_{26}−C_{28} triaromatic steroids are valid before PM 8. Therefore, using PAH-based parameters in the geochemical assessment of in-reservoir biodegraded or oil sands should be done with care, and the relative biodegradation susceptibilities of related components should be taken into consideration.

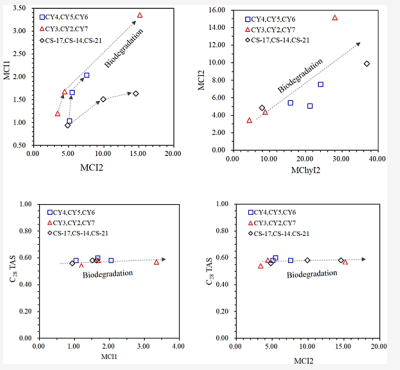

KEYWORDS: *polycyclic aromatic hydrocarbons, biodegradation, crude oil and oil sand, maturity, Junggar Basin*

1. INTRODUCTION

Polycyclic aromatic hydrocarbons (PAHs) are important constituents of crude oils, representing typically 20−45% of the total hydrocarbons.[1] PAHs have been applied as molecular maturity parameters on the basis of the different thermodynamic stabilities of individual isomers,[2−11] for example, MDR = 4-methylDBT/1-methylDBT,[2] DMDBTI = (4,6-+2,4-DMDBT)/(1,4-+1,6+1,8-+4,6-+2,4-DMDBT),[3] TMDBTI = 2,4,6-TMDBT/(2,4,7-+2,4,8-TMDBT),[4] MCI1 = 1.5 × (2-MChy + 3-MChy)/(chrysene + 1-MChy + 4-MChy + 5-MChy + 6-MChy),[5] MPYR [2-MPy/(2-MPy + 1-MPy)],[3] TAS = (C_{20} + C_{21} triaromatic steroids)/(C_{20} + C_{21} + C_{26} + C_{27} + C_{28} triaromatic steroids),[6] C_{28} TAS = C_{28} triaromatic steroid 20S/(20S + 20R).[7] In addition, PAHs are also applied to oil−oil/source rock correlation, depositional environment reconstruction, and oil migration pathway tracing.[3,12−19] For example, it is well accepted that the relative abundance of dibenzothiophenes is largely controlled by depositional conditions, and it can serve as a good indicator to distinguish depositional environments and correlate oils.[12] However, secondary alteration processes, such as biodegradation and water washing, can also change the content and composition of PAHs in crude oils, resulting in the failure of geochemical indicators. The amount of biodegradable crude oil may exceed the amount of conventional crude oil in the world.[7] Therefore, it is very essential to develop a better understanding of the biodegradation of PAHs to reduce their effects on the biomarker indicators that are used for oil and source rock research.

Previous studies have investigated the microbial biodegradation of PAHs, including biodegradation susceptibility and biodegradation pathways.[20−25] The latter includes at least two major aspects: the oxidation of aromatic ring carbons and alkyl carbons.[26−28] Therefore, different molecular structures of each homologous compound may possess a different susceptibility to biodegradation. To describe the extent of biodegradation,

Received: December 7, 2022
Revised: February 15, 2023
Accepted: March 13, 2023
Published: March 23, 2023

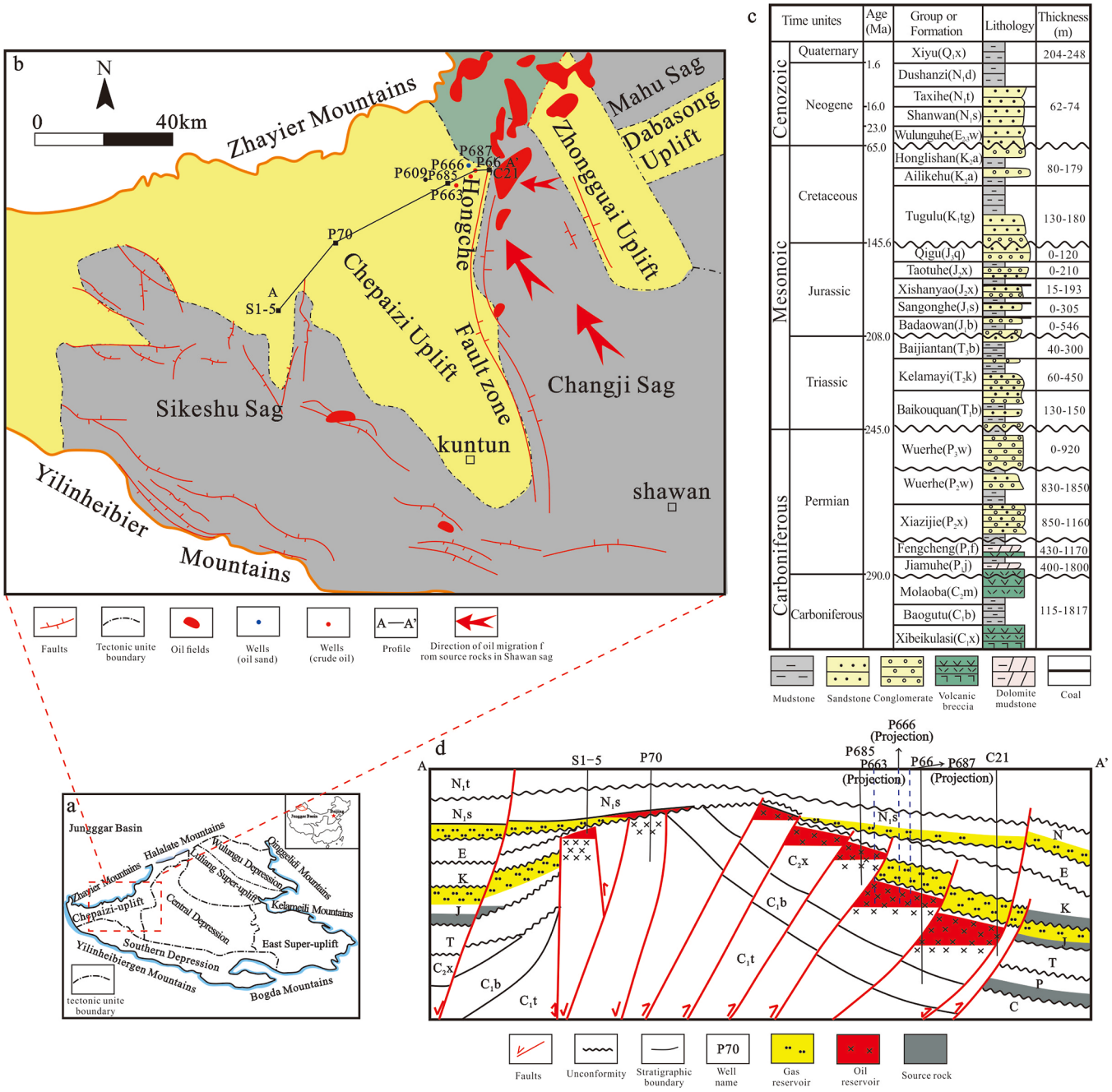

Figure 1. Location of the Junggar Basin in China (a), structural units and location of the Chepaizi Uplift and the studied crude oil and oil sand samples in the Junggar Basin (b), simplified stratigraphic column of the northwestern Junggar Basin (c), geological section of the Chepaizi Uplift trending SW–NE (d).

several assessment rankings have been established,[29−33] among which the most widely used was proposed by Peters and Moldowan[29] and involved PM 1 (the least biodegradation) to PM 10 (the severest biodegradation). The environment and related make-up of the microbial community have major impacts on the relative rates of biodegradation of the different hydrocarbon substrates, most significantly between aerobic and anaerobic communities.[23,34,35] Therefore, seeking an absolute, universal correlation between the PM scale, which uses only saturated hydrocarbons, and PAH biodegradation is likely to be elusive. Moreover, the extent of PAH biodegradation has not been well correlated with PM levels except for naphthalenes and phenanthrenes. It is widely accepted that the biodegradation of PAHs depends on their molecular structures, such as the number of aromatic rings and the degree of alkylation. Generally, the rate of biodegradation decreases with the increasing number of aromatic and alkyl substituents.[20,36,37] In addition, the position of alkyl substituents is a critical factor in the biodegradation rate. For example, 9-methylphenanthrene (9-MP) is the most resistant MP isomer to both naturally biodegradable oils and laboratory experiments.[38−40] In addition, 1,7-dimethylphenanthrene (1,7-DMP) is the most vulnerable component, while 1,3-+3,9-+2,10-+3,10-DMP is the most recalcitrant component.[23] As is the case for alkylnaphthalenes, researchers have reported that

https://doi.org/10.1021/acsearthspacechem.2c00378
ACS Earth Space Chem. 2023, 7, 823−837

isomers with methyl substituents at the 1 and 6 positions are less resistant to biodegradation.[22]

It seems that the order of alteration of different saturated hydrocarbons is clear, and a quasi-systematic classification scheme has been established.[29] However, PAHs have rarely been involved in these scales, especially those that were used in the evaluated parameters, such as dibenzothiophene, chrysene and their alkylated homologues. The order of susceptibility to microbial attacks of each individual compound is not explicit. In this study, we present the relative abundance of dibenzothiophenes, fluorenes, chrysenes, pyrenes, and triaromatic steroid hydrocarbons in less biodegraded and more severely biodegraded crude oil and oil sands from the Chepaizi Uplift, Junggar Basin, NW China. The main aims of this study are (1) to identify the relative susceptibilities to biodegradation of less studied PAH classes in severe biodegradation cases and (2) to elucidate the implications for maturity parameter applications.

2. GEOLOGICAL SETTING

The Chepaizi Uplift is close to the northwestern Junggar Basin. The shape of the Chepaizi Uplift is a triangle in plane. It is close to the Changji Sag and Zhongguai Uplift to the east, the Sikeshu Sag to the south, and the Zhayier Mountain to the northwest (Figure 1). It has experienced the Hercynian, Indosinian, Yanshanian, and Himalayan tectonic events since the late Paleozoic.[41] Its evolution mainly involved three stages: intense uplift, and slow and rapid subsidence. The Chepaizi Uplift is an inherited paleohigh, with the important Hongche Fault Belt and a series of low-angle thrust faults resulting from the Hercynian tectonic movement. In most areas, Permian, Triassic, and Jurassic deposits are lacking, and only thin strata were deposited near the Hongche Fault.

The Carboniferous volcanic rocks in the east wing of the Chepaizi Uplift have been an important exploration target in recent years. The Changji Sag and Sikeshu Sag are the main two surrounding generative source kitchens for the Chepaizi Uplift, and Carboniferous crude oils of the eastern Chepaizi Uplift that had been biodegraded at different levels were derived mainly from the Permian source rocks of the Changji Sag owing to the widely distributed faults.[42,43]

3. SAMPLES AND METHODS

3.1. Samples. Six crude oil and three oil sand samples which underwent varying extents of biodegradation were collected from the Chepaizi Uplift, Junggar Basin, NW China (Figure 1). Petroleum exploration revealed that oil and gas distribution patterns were controlled by the large-scale thrust fault system in this region.[44,45] The study samples are all from the Carboniferous strata. The depths of the oil sand samples are 1003.01, 982.24, and 1238.6 m. Crude oils are heavy oils with densities ranging from 0.9285 to 0.9480 g/cm^3 and viscosities ranging from 174 to 2426 mPa·s. The effects of biodegradation on PAHs were investigated. Geochemical investigation indicates that they are all of the typical lacustrine origin and are derived from the Permian source rocks.[46]

3.2. Separation of Petroleum Fractions. The oil sand samples were extracted with an azeotropic mixture of dichloromethane (DCM)/methanol (CH_3OH) (93:7, v/v) via Soxhlet extraction for 48 h. The extractable organic matter and crude oils were de-asphalted by precipitation with excess *n*-hexane. Then the saturated, aromatic, and resin fractions were separated by liquid chromatography on a silicagel/alumina oxide column using petroleum ether, DCM/petroleum ether (2:1, v/v), and DCM/ethanol (1:1, v/v), respectively.

3.3. Gas Chromatography−Mass Spectrometry. The gas chromatography−mass spectrometry (GC−MS) analysis of saturated hydrocarbon and aromatic hydrocarbon fractions was conducted on Agilent 6890 gas chromatography coupled to an Agilent 5975 mass selective detector and equipped with a HP-5MS elastic quartz capillary column (column length: 60 m, internal diameter: 0.25 mm, film thickness: 0.25 μm). Ultrahigh-purity helium was used as the carrier gas at a flow rate of 1 mL/min (70 eV ionization energy). The temperature of the sample inlet was maintained at 300 °C. The temperature of the GC oven for analyzing saturated hydrocarbons was set at 50 °C for 1 min, then programed from 50 to 120 °C at 20 °C/min, from 120 to 250 °C at 4 °C/min, then programed from 250 to 310 °C at 3 °C/min, and held for 30 min at 310 °C. The GC oven temperature for analyzing aromatic hydrocarbons was initially set to 80 °C, gradually increased to 310 °C at 3 °C/min, and held at 310 °C for 20 min. The MS was scanned from m/z 50 to 550 using both selective ion monitoring (SIM) mode and the total ion current (TIC) to analyze the distributions of the aliphatic and aromatic hydrocarbons. The relative abundance of the studied compounds was analyzed and calculated using SIM mode.

4. RESULTS AND DISCUSSION

4.1. Hydrocarbons and Biodegradation. Total ion chromatograms (TICs) of saturated hydrocarbons possess a typical marker of oil biodegradation, which has an obvious unresolved complex mixture and removal of *n*-alkanes. *n*-Alkanes are the most susceptible components to biodegradation.[8,30,36] In the CY6 oil sample, the *n*-alkanes have been completely removed, and trace acyclic isoprenoids remain. Its petroleum degradation level is greater than that of PM 6 with the widespread presence of 25-norhopanes.[29]

From the mass chromatograms (m/z 191) (Figure 2), we find that 17α(H) hopane (C_{30}H) is the dominant component among the pentacyclic terpanes except the CY6 oil sample, and C_{31}−C_{35} homohopanes are present in minor amounts. However, the C_{29} 17α(H),21β(H) 25-norhopane was detected. When heavily degraded, demethylation of hopanes occurs to form 25-norhopanes,[47] although some research shows that biodegradation of hopanes does not always yield 25-norhopanes.[48,49] Additionally, the ratio of 25-norhopane to 25-norhopane plus 17α(H) hopane (C_{30}H) increases with the increasing degree of biodegradation in CY4, CY5, and CY6 oil samples (Table 1), which results from the removal of the methyl group from the C-10 position in hopanes and the formation of 25-norhopane. Tricyclic terpanes (i.e., cheilanthanes, referred to here after as TTs) have been enriched relative to their high abundance over hopanes due to biodegradation.

Tricyclic terpanes (TTs) are more resistant than regular steranes and hopanes. Cheng[25] proposed that the relative susceptibility of TTs to biodegradation decreases with increasing carbon number except for C_{20}TT. Our results show that C_{21}TT, C_{23}TT, and tetracyclic terpanes are well preserved through biodegradation. It has been proposed that demethylated tricyclic terpanes are the products of biodegradation and are formed by the microbial removal of the methyl group at C-10 in tricyclic terpanes.[39,50] In our studies, only trace C_{19}NTT, C_{22}NTT, and C_{23}NTT have been detected with hopanes and regular steranes were either partially or completely removed. This is consistent with previous research studies.[51,52]

https://doi.org/10.1021/acsearthspacechem.2c00378
ACS Earth Space Chem. 2023, 7, 823−837

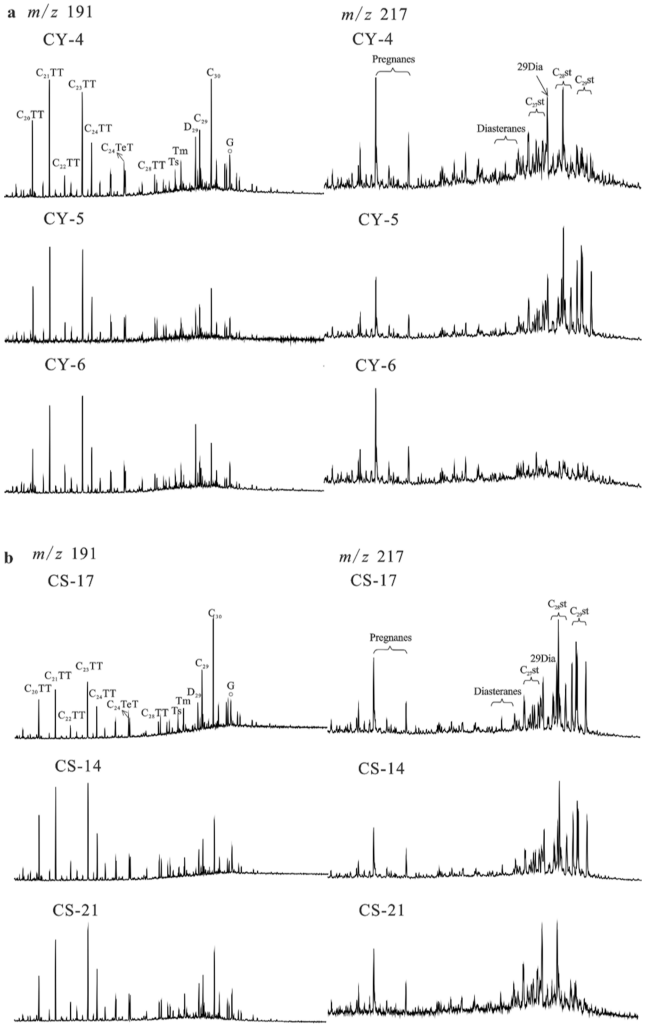

Figure 2. Representative mass chromatograms (m/z 191 and m/z 217) showing the distributions of tricyclic diterpanes, pentacyclic triterpanes (left), and steranes (right) in crude oils and oil sands with different extents of biodegradation from the Chepaizi Uplift, Junggar Basin, NW China. C_{20}−C_{26}TT: C_{20}−C_{28} tricyclic terpanes; C_{24}TeT: C_{24} tetracyclic terpanes; Ts: 18α-trisnorneohopane; Tm: 17α-trisnorhopane; D_{29}: C_{29} 25-norhopane; C_{29}−C_{30}: C_{29}−C_{30} hopanes; G: gammacerane; 29Dia: C_{29} diasteranes; C_{27}−C_{29} st: C_{27}−C_{29} steranes.

Cheilanthanes are attacked while regular hopanes are still present, but at a lower rate. With elevated biodegradation (from CY-4 to CY-6), the relative enrichment of C_{21}TT decreases whereas the relative abundance of C_{23}TT increases. Moreover, the relative abundance of C_{20}TT also appears to decrease (Figure 2a,b).

In this study, regular steranes were observed in most altered samples. However, there was some biodegradation of steranes, which was evidenced by the relative increase of C_{21}−C_{22} steranes (Pregs) (Figure 3). Diasteranes and C_{21}−C_{22} steranes

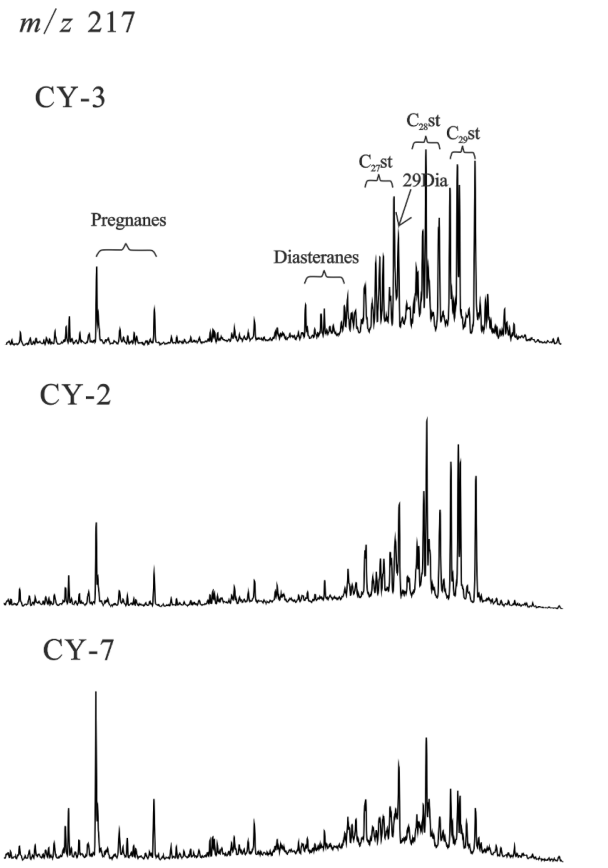

Figure 3. Representative mass chromatograms (m/z 217) showing the distributions of steranes in crude oils with different extents of biodegradation from the Chepaizi Uplift, Junggar Basin, NW China. 29Dia: C_{29} diasteranes; C_{27}−C_{29} st: C_{27}−C_{29} steranes.

seemed to be unaffected in all examined samples. In samples CS-17 and CS-14, the C_{27}−C_{29} regular steranes seem to be unaltered, but in sample CS-21, the C_{29} regular steranes were

Table 1. Geochemical Parameters of the Representative Crude Oil and Oil Sand Samples[a]

sample ID	type	well	depth (m)	C_{28} TAS	$D_{29}/(C_{30}H + D_{29})$	$G/C_{31}H$	Preg/St	TT/H	$C_{23}TT/C_{21}TT$	PM
CS-17	oil sand	P666	1003.01	0.55	0.23	0.74	0.09	0.79	1.18	6
CS-14	oil sand	P666	982.24	0.56	0.34	1.03	0.13	1.27	1.02	6
CS-21	oil sand	P666	1238.6	0.56	0.43	1.03	0.24	1.30	1.16	7
CY3	crude oil	P666		0.54	0.16	0.50	0.06	0.48	1.04	6
CY2	crude oil	P66		0.56	0.12	0.56	0.09	0.69	1.03	6
CY7	crude oil	P687		0.56	0.11	0.57	0.41	1.15	0.89	7
CY4	crude oil	P66		0.56	0.31	0.96	0.30	0.93	0.92	7
CY5	crude oil	P66		0.59	0.35	1.01	0.11	1.94	0.95	6
CY6	crude oil	P663		0.56	0.57	1.60	0.69	1.51	1.11	8

[a]Abbreviations: C_{28} TAS = C_{28} triaromatic steroid 20S/(20S + 20R); $D_{29}/(C_{30}H + D_{29})$ = C_{29} 25-norhopane/(C_{30} hopane + C_{29} 25-norhopane); $G/C_{31}H$ = gammacerane/C_{31} hopane; Preg/St = pregnanes/steranes; TT/H = tricyclic terpanes/hopanes; $C_{23}TT/C_{21}TT$ = C_{23} tricyclic terpanes/C_{21} tricyclic terpanes; PM = Peters and Moldowan scale.

https://doi.org/10.1021/acsearthspacechem.2c00378
ACS Earth Space Chem. 2023, 7, 823−837

almost completely removed, and the C_{29} diasterane became the dominant component among them. In the CY4 and CY7 oils, C_{29} 5α(H),14α(H),17α(H),20*R*-24-ethyl-cholestane and C_{28} 5α(H),14α(H),17α(H),20*R*-24-methyl-cholestane were evidently degraded over their 20S isomers. In the CY6 oil, most steranes had been removed, leaving Pregs as the dominant component. Therefore, the assumed unaltered Pregs can also serve as an "internal standard" for assessing the relative biodegradation level in our samples (Table 1).[53]

4.2. Determining the Levels of Biodegradation. Biodegradation has noteworthy effects on chemical composition and is well known as a "quasi-stepwise" process.[54] The biodegradation of hydrocarbons occurs in reservoirs or surface spills simultaneously, but the biodegradation rate of individual components is different, reflecting their different susceptibilities to biodegradation. And based on this, some particular molecular parameters can be used to determine the level of biodegradation. One difficulty is that the initially charged oil is degraded, but the later charged oil is lightly degraded or nondegraded, resulting in the co-occurrence of 25-norhopanes and *n*-alkanes. Due to multistage oil charging, the oil column may be a mixed product that was expelled from different source rocks over a considerable maturity range. The total ion chromatograms (TICs) of saturate fractions in this study show most *n*-alkanes have been removed, which suggests that there are hardly any fresh oil charges or that the minor charge of fresh oil does not shadow the effects of biodegradation. Previously completed studies have demonstrated that the Carboniferous heavy oils in the eastern Chepaizi area were mostly derived from Permian source rock in the Changji Sag.[42,43,55] In addition, the distribution of C_{26}−C_{28} triaromatic steroids has high similarities, which suggests a single source origin (Figure S1). The values of the C_{28} triaromatic steroid 20S/(20S + 20R) also point to a similar maturity of the study samples.

According to the PM level proposed by Peters and Moldowan,[29] the occurrence of the 25-norhopane series of all samples at *m*/*z* 177 indicates biodegradation to PM 6. The ratio of $D_{29}/(C_{30}H + D_{29})$ ranges from 0.23 to 0.43 in oil sands and from 0.31 to 0.57 in CY4, CY5, and CY6 oils, respectively, suggesting increasing biodegradation. This is contrary to CY3, CY2, and CY7, which may result from the biodegradation of C_{29} 25-norhopane or no formation of C_{29} 25-norhopane. Similarly, the ratios of gammacerane/C_{31}, 17α-hopane, and Preg/St also increase in these sample sequences. The severe biodegradation of steranes in CS-21, CY7, and CY4 samples indicates their Peters and Moldowan level 7 (PM 7). For CY6, the dominance of C_{29} 25-norhopane and the removal of C_{29} diasteranes indicate its biodegradation to PM 8. Taking all parameters into consideration, the relative biodegradation degrees of these samples can be determined as listed in Table 1. An abnormity is that the depletion of steranes in CY4 oil is greater than that in CY5 oil, but other parameters, including the phenanthrene series (Figure 4), suggest that CY5 oil is more severely degraded. Therefore, we deduce that the lower removal of steranes in the mass chromatograms (*m*/*z* 217) is the result of the minor recharging of fresh oil. Based on the above discussion, we conclude that the biodegradation levels of the three groups follow the following order: CY3 < CY2 < CY7, CY4 < CY5 < CY6, and CS-17 < CS-4 < CS-21.

4.3. Biodegradation Effects on Polycyclic Aromatic Hydrocarbons. *4.3.1. Dibenzothiophenes.* Generally, the more alkylated aromatic hydrocarbons that are present, the more resistant they are to biodegradation, as verified by Mazeas.[56] In this study, the relative abundance of dibenzothiophene (DBT), 4-methyldibenzothiophene (4-MDBT), and 2-+3-methyldibenzothiophene (2-+3-MDBT) gradually decrease while that of 1-methyldibenzothiophene (1-MDBT) increase during biodegradation. It can be easily concluded that 1-MDBT is more resistant to biodegradation than other methyldibenzothiophene isomers. The rate of dibenzothiophene depletion is higher than that of 4-MDBT and 2-+3-MDBT, indicating that it is the most susceptible compound compared with methyldibenzothiophenes. There is no evident depletion of 4-MDBT and 2-+3-MDBT in Figure 5, suggesting their lower susceptibilities to biodegradation, and 4-MDBT is more preferential to biodegradation than 2-+3-MDBT. In addition, some abnormities (such as the unaltered relative abundance of DBT in Figure 5b) may occur as a result of other alterations, such as water washing and secondary charging. The susceptibilities to biodegradation thus follow the following order: DBT > 2-+3-MDBT > 4-MDBT ≫ 1-MDBT.

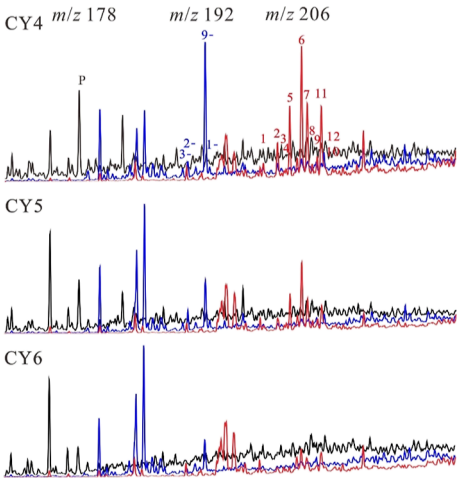

Figure 4. Representative summed mass chromatograms of phenanthrene and alkylphenanthrenes (*m*/*z* 178, 192, and 206) in the studied oils from the Junggar Basin. P: phenanthrene; 3-: 3-methylphenanthrene (MP); 1: 3-ethylphenanthrene (EP); 2: 2-EP + 3,6-dimethylphenanthrene (DMP); 3: 9-EP + DMP; 4: 1-EP + 2,6+3,5-DMP; 5: 2,7-DMP; 6: 2,10+1,3+3,10+3,9-DMP; 7: 1,6+2,9+2,5-DMP; 8: 1,7-DMP; 9: 2,3-DMP; 10: 4,9+4,10+1,9-DMP; 11: 1,8-DMP; 12: 1,2-DMP.

Because oil samples were severely degraded, only traces of dimethyldibenzothiophenes were detected except in CY3 oil. However, the gas chromatogram of oil sands reveals that dimethyldibenzothiophenes are more refractory than dibenzothiophene and methyldibenzothiophenes (Figure S2). The bar chart (Figure 4c) reveals obvious relative increases in 4,6-dimethyldibenzothiophene (4,6-DMDBT) and 4-ethyldibenzothiophene (4-EDBT), which indicates that they are more resistant to biodegradation than other DMDBTs. In contrast, the relative abundances of 2,4-dimethyldibenzothiophene (2,4-DMDBT), 2,6-dimethyldibenzothiophene (2,6-DMDBT), 3,7-dimethyldibenzothiophene (3,7-DMDBT), 1,4+1,6+1,8-dimethyldibenzothiophene (1,4+1,6+1,8-DMDBT), and 1,3-+1,9-dimethyldibenzothiophene (1,3-+1,9-DMDBT) show relatively decreasing trends at different rates with increasing biodegradation compared to 4,6-DMDBT and 4-EDBT. According to these trends, we can easily infer the relative susceptibilities of C_2-dibenzothiophenes to microbial attack as follows: 3,7-DMDBT > 2,4-DMDBT ~ 2,6-DMDBT > 1,3-+1,9-DMDBT > 1,4-+1,6-

https://doi.org/10.1021/acsearthspacechem.2c00378
ACS Earth Space Chem. 2023, 7, 823−837

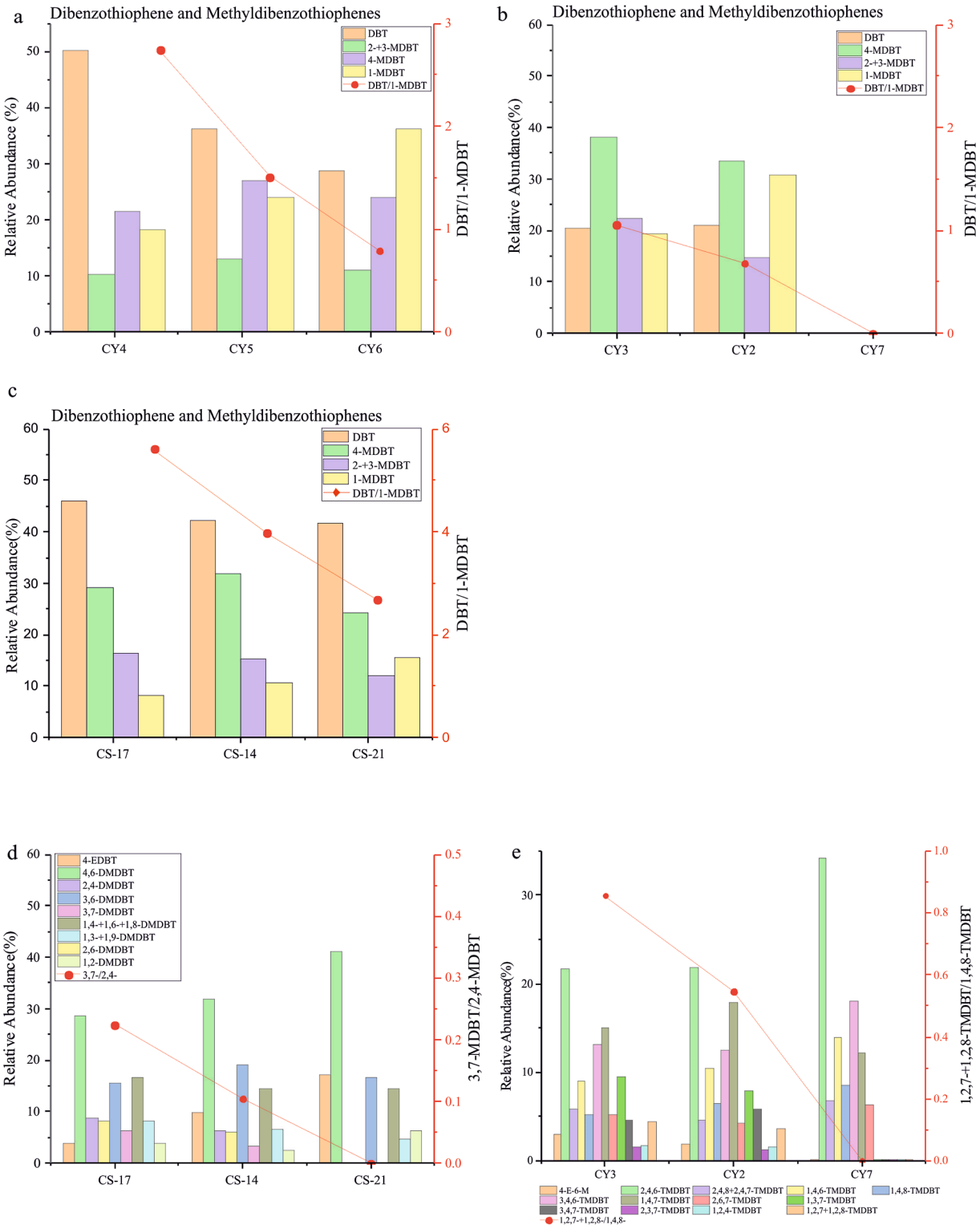

Figure 5. Bar graphs showing the relative abundance (%) of components in crude oils from the Chepaizi Uplift, Junggar Basin with increasing biodegradation: (a−c) dibenzothiophene (DBT) and methyldibenzothiophenes (MDBT); (d) C_2-dibenzothiophenes. DMDBT: dimethyldibenzothiophene; EDBT: ethyldibenzothiophene. (e) C_3-Dibenzothiophenes. TMDBT: trimethyldibenzothiophene; 4-E-6-M: 4-ethyl-6-methyldibenzothiophene. The relative abundance of a compound is calculated by taking the total abundance of the compounds as 100%, e.g., the sum of DBT and DMDBT equals 100% in each crude oil.

+1,8-DMDBT > 3,6-DMDBT > 1,2-DMDBT > 4-EDBT > 4,6-DMDBT.

The detectable peaks of trimethyldibenzothiophene isomers in the other two groups are of very low relative intensity. In the CY3, CY2, and CY7 oils, the relative abundances of 4-ethyl-6-methyldibenzothiophene (4-E,6-MDBT), 1,3,7-trimethyldibenzothiophene (1,3,7-TMDBT), and 1,2,7-+1,2,8-trimethyldibenzothiophene (1,2,7-+1,2,8-TMDBT) decrease slightly with an

https://doi.org/10.1021/acsearthspacechem.2c00378
ACS Earth Space Chem. 2023, 7, 823−837

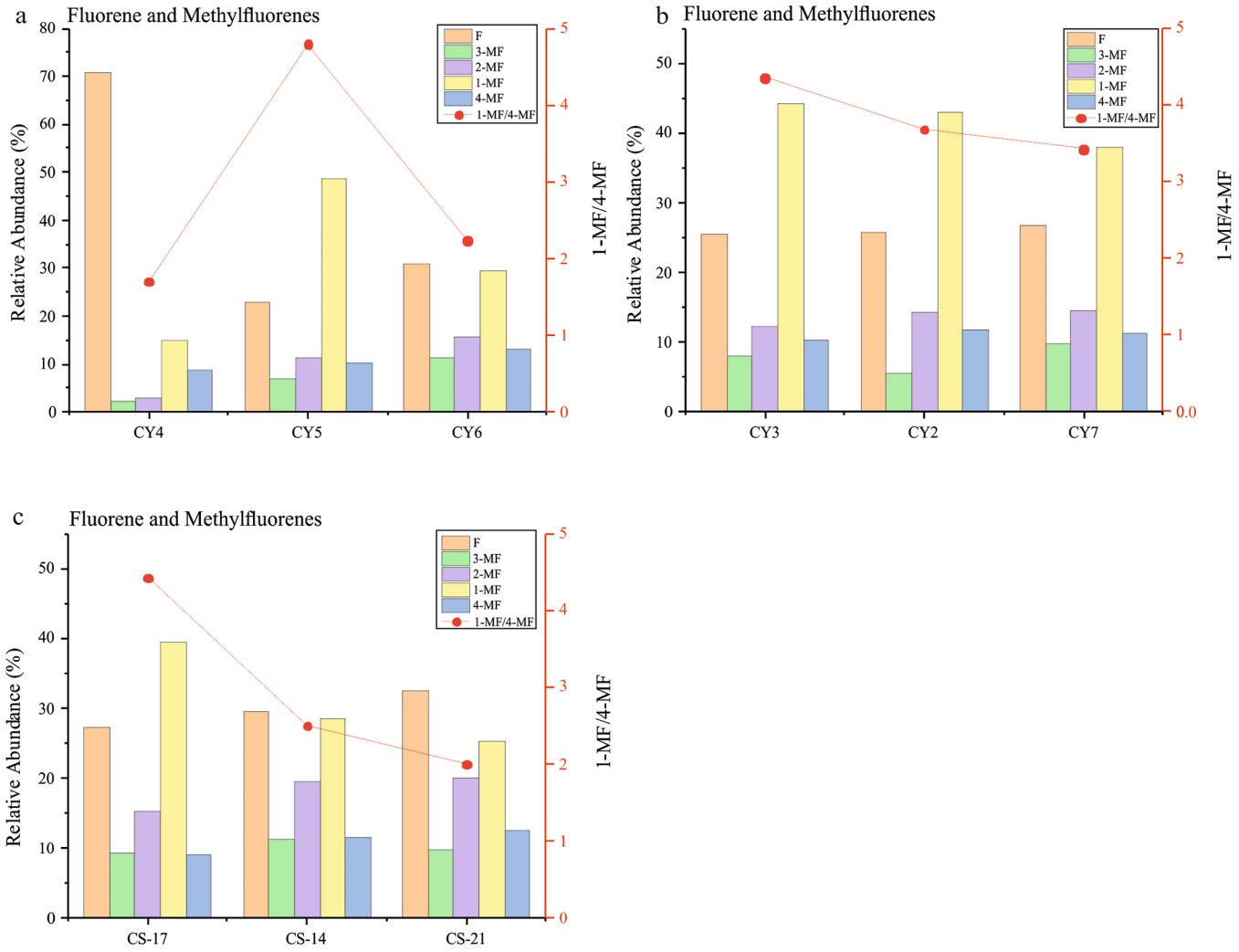

Figure 6. Bar graphs showing the relative abundance (%) of components in crude oils (a,b) and oil sands (c) from the Chepaizi Uplift, Junggar Basin with increasing biodegradation: fluorenes (F) and methylfluorenes (MF).

increasing degree of biodegradation while those of 2,4,6-trimethyldibenzothiophene (2,4,6-TMDBT), 1,4,6-trimethyldibenzothiophene (1,4,6-TMDBT), 3,4,6-trimethyldibenzothiophene (3,4,6-TMDBT), and 1,4,8-trimethyldibenzothiophene (1,4,8-TMDBT) increase, and there is less variation in the of relative abundance for 1,2,4-trimethyldibenzothiophene (1,2,4-TMDBT) and 2,3,7-trimethyldibenzothiophene (2,3,7-TMDBT). These variations in individual isomers indicate their relative susceptibilities to biodegradation. Therefore, we can infer that the TMDBT isomer order for the susceptibility to biodegradation is as follows: 1,2,7-+1,2,8-TMDBT > 1,3,7-TMDBT > 4-E,6-MDBT > 1,2,4-TMDBT > 1,4,8-TMDBT > 1,4,6-TMDBT > 3,4,6-TMDBT > 2,4,6-TMDBT.

4.3.2. Fluorenes. Generally, the susceptibility of non-alkylated aromatic compounds and their alkylated homologues to biodegradation decreases as the number of alkyl substituents on aromatic rings increases.[57] However, fluorene biodegraded more slowly than methylfluorene in our study, suggesting that demethylation may be an important step in aromatic hydrocarbon biodegradation under some circumstances. Because of the salient divergence of one compound (e.g., fluorene in CY4), the changing trends of other compounds may be overprinted. However, when conducting comprehensive analyses on all groups of samples, we can still find that the relative abundance of fluorene and 1-MF showed a downward trend while that of other methylfluorenes are opposite (Figure 6). These contrary trends indicate that the former is more easily degraded than the latter. In combination with their altered rates, the order of susceptibilities to biodegradation of fluorene and methylfluorenes is concluded in the following order: 1-MF > F > 2-MF > 3-MF > 4-MF.

For C_2-methylfluorenes (peaks A and B are unspecified C_2-methylfluorenes, Figure S3), the varied biodegradation tendency of the oil groups and oil sand group is somewhat different (Figure 7). The most salient conflict exists between compound 1,7-DMF and 1,6-DMF. The relative abundance of compound 1,7-DMF in oil sands decreases rapidly during biodegradation, while that of compound 1,6-DMF increases abruptly. The opposite is true for the oil samples. This may result from their different environmental conditions, such as oxygen availability, different types of bacteria, oil-sand surface adsorption effects and/or temperature. In crude oils, compounds 1,8-DMF and 1,6-DMF gradually decreased, while compounds 1,7-DMF, E and F decreased during biodegradation (Figure 7a,b), indicating that the former is more susceptible to biodegradation than the latter. According to the rates of compound variation, we can conclude that their susceptibilities to biodegradation in crude oils are in the following order: 1,6-

https://doi.org/10.1021/acsearthspacechem.2c00378
ACS Earth Space Chem. 2023, 7, 823−837

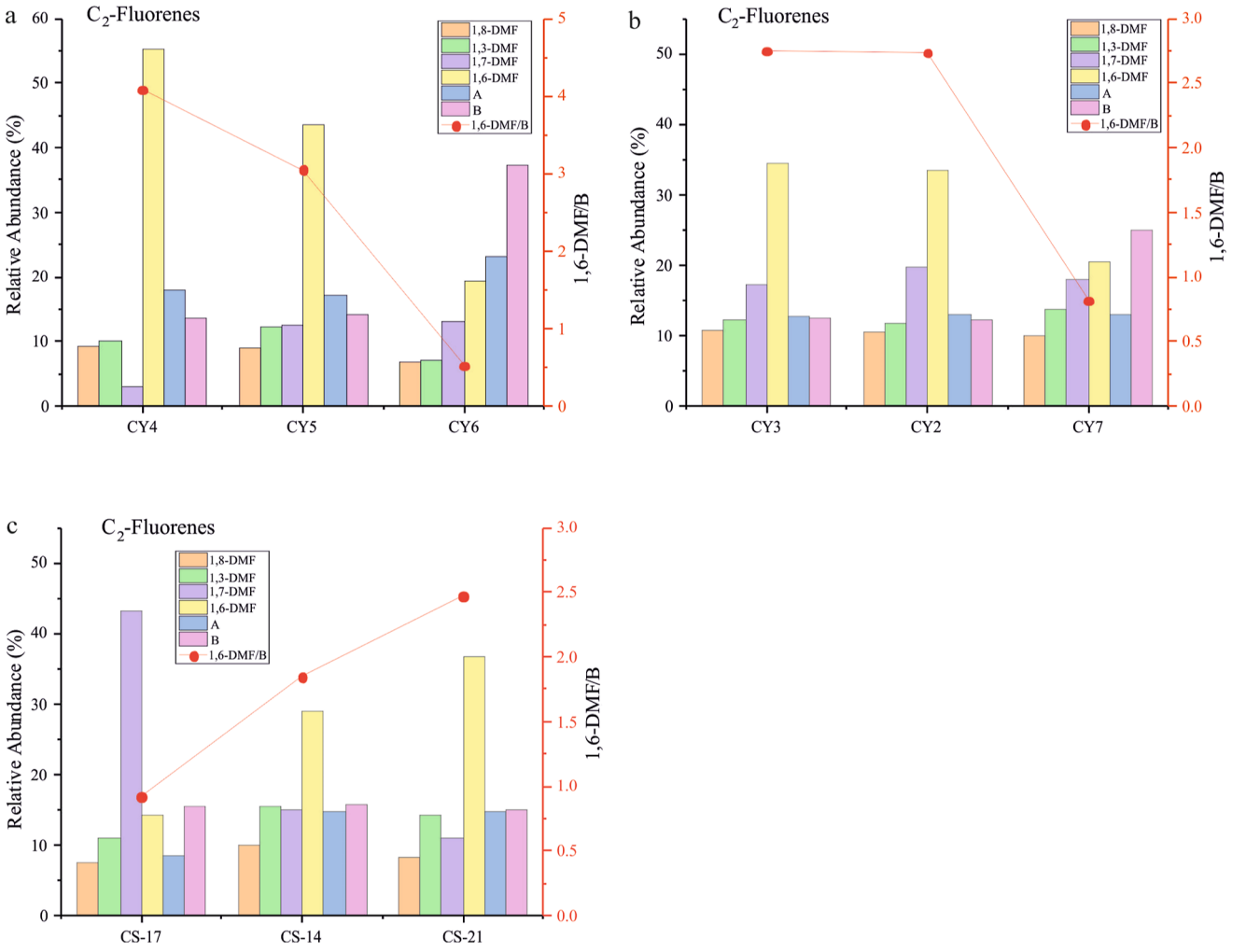

Figure 7. Bar graphs showing the relative abundance (%) of components in crude oils (a,b) and oil sands (c) from the Chepaizi Uplift, Junggar Basin with increasing biodegradation: C_2-fluorenes.

DMF > 1,8-DMF > 1,3-DMF > 1,7-DMF ∼ A > B. In oil sands, the order is slightly different: 1,7-DMF > B > 1,8-DMF > A ∼ 1,3-DMF > 1,6-DMF.

4.3.3. Chrysenes. For crude oil samples, there is an obvious increasing trend for 3-MCh, while chrysene and other methylchrysenes generally decrease in relative abundance as biodegradation increases (Figures 8 and S4). In the most severely degraded CY7 oil, 3-MCh becomes the dominant compound among methylchrysenes. Similarly, in the less degraded oil sands, the pattern of change in relative abundance is not obvious but does exist (Figure 8). From these observations, we can conclude that 3-MCh has a higher resistance to biodegradation than chrysene and other methylchrysenes. Chrysene is more susceptible to biodegradation, as evidenced by its higher depletion rate than 2-MCh, 4-+6-MCh, and 1-MCh (Figure 8). Compared with the less degraded oil sands, the relative abundance of chrysene and 3-MCh in the severely degraded oil groups changed obviously, indicating that they are resistant to biodegradation and can be used for assessing more severe biodegradation. Moreover, in severely biodegraded circumstances (PM levels 6−8), they are more reliable for evaluating the biodegradation influence than hopanes and steranes, which are largely controlled by the source input and maturity in different petroleum systems.[33] The 3-MCh ratio in whole methylchrysenes (3-MCh/∑MCh) proposed by Huang[33] gradually increases with increasing biodegradation in our studied samples, which is consistent with their conclusion. Based on our observations, we suggest that the susceptibilities of chrysene and methylchrysene to biodegradation are as follows: 2-MCh ∼ 1-MCh > 4-+6-MCh > chrysene ≫ 3-MCh.

4.3.4. Pyrenes. The relative abundance of pyrene and its alkylated homologues shows a slight change in oil sands (Figure S5), because their biodegradation levels are lower than those of crude oil samples, which indicates that the pyrenes are more refractory to biodegradation than the other PAHs mentioned above. However, in the severely biodegraded crude oil samples (Figure 9), the relative decrease in pyrene and 2-MPy and increase in 4-MPy and 1-MPy, when combined with their variation rates, suggest their susceptibility order to biodegradation as follows: pyrene > 2-MPy > 4-MPy > 1-MPy.

4.3.5. Triaromatic Steroid Hydrocarbons. It is well accepted that TAS are more resistant to biodegradation than other PAHs. The C_{20-21} triaromatic steroids are preferentially removed over the high molecular weight triaromatic steroid hydrocarbons.[20,58] However, this occurs only in severely biodegraded oils (CY6 and CS-21). In our study, C_{21-22} methyltriaromatic steroids are slightly degraded in crude oil group CY4−CY6 and oil sand CS-21, while triaromatic steroids remain unchanged. On the other hand, biodegradation can result in a greater degradation of the C_{26}20S TAS compared with its higher homologues.[39,58] The

https://doi.org/10.1021/acsearthspacechem.2c00378
ACS Earth Space Chem. 2023, 7, 823−837

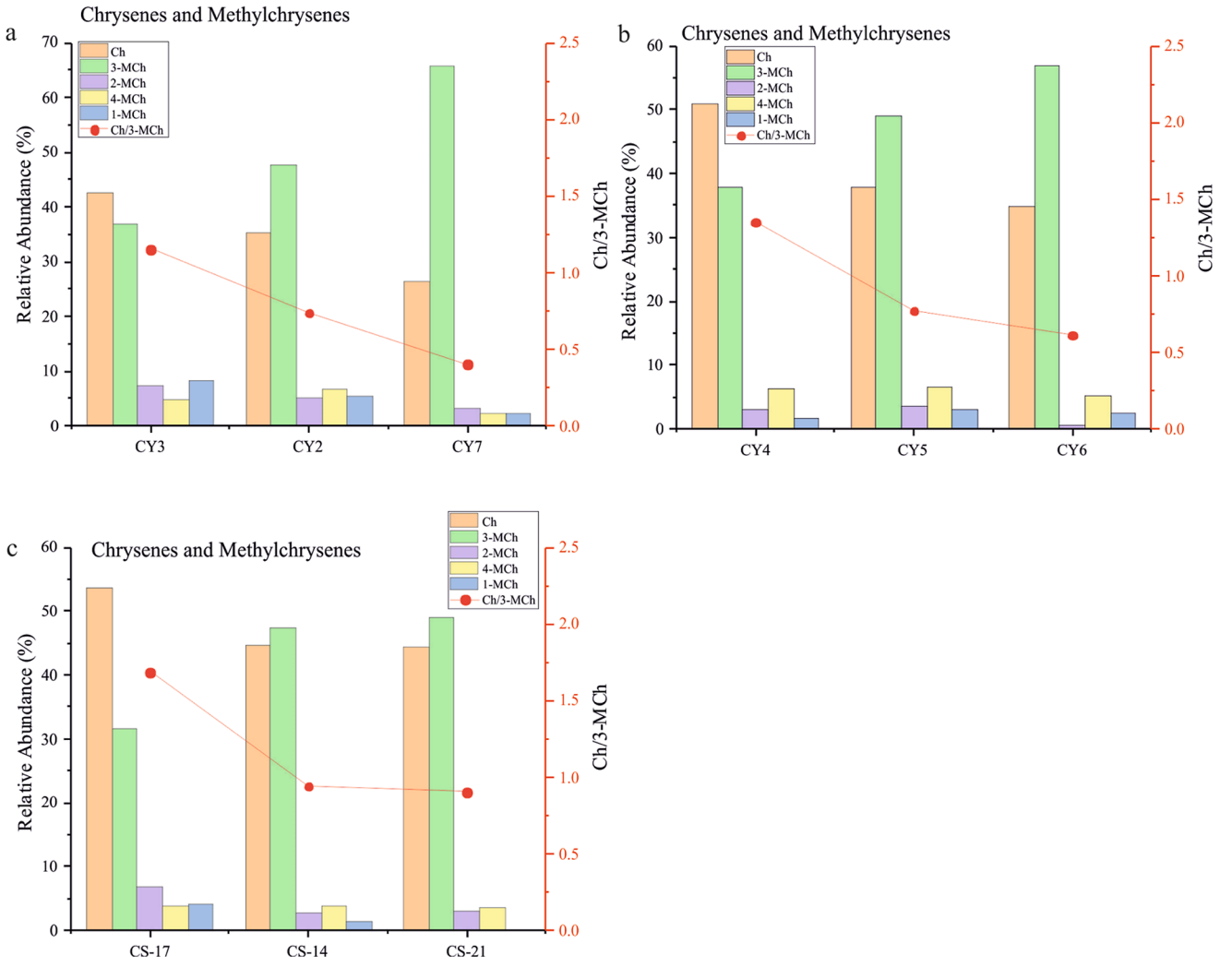

Figure 8. Bar graphs showing the relative abundance (%) of components in crude oils (a,b) and oil sands (c) from the Chepaizi Uplift, Junggar Basin with increasing biodegradation: chrysene (Ch) and methlchrysenes (MCh).

preferential depletion of C_{26}20S TAS is shown in bar graphs (Figure 10). The relative abundances of C_{27}20R TAS and C_{28}20R TAS remain almost constant. The relative abundance of C_{26}20R+C_{27}20S TAS presents a slight reduction while that of C_{28}20S TAS shows a slight increase, which indicates their relative susceptibilities to biodegradation: C_{26}20S TAS > C_{26}20R+C_{27}20S TAS > C_{27}20R TAS ∼ C_{28}20R TAS > C_{28}20S TAS.

The relative susceptibilities to the biodegradation of individual compounds within each PAH series are assessed and summarized in Table 2. Based on their relative susceptibilities to biodegradation, the relevant biodegradation assessment parameters are listed in Table 2.

4.4. Implication of Biodegradation Effects on PAHs. Saturated and aromatic hydrocarbons are the basic constituents for geochemical studies in many respects, including maturation assessment, depositional environment reconstruction, and oil migration pathway indication. However, biodegradation can largely alter hydrocarbon compositions, which affect geochemical parameters. Generally, the biodegradation of PAHs (but not triaromatic and monoaromatic steroids) occurs when oils are slightly or heavily biodegraded, prior to significant attack by resistant tricyclic terpanes and pregnanes. Our study shows that there is no regular relationship between the susceptibility to biodegradation and the thermostability of individual components. This indicates that the microbial attack to them is related to their stereochemical structure. Therefore, it invalidates most maturity parameters. The relevant PAH maturity parameters are listed in Table 3. As mentioned above, most saturated hydrocarbons and PAHs have suffered biodegradation up to PM 8, except triaromatic steroids. In this stage, the reliable PAH maturity parameter is the C_{28} triaromatic steroid ratio 20S/(20S + 20R), which is rarely attacked by microorganisms. This parameter indicates that thermal maturity lies within a very narrow range in our samples, suggesting that the study oils were generated from source rocks during the early oil generation stage. Other parameters, such as MPI1, MDR, and MPYR (Table 3), are no longer useful as a result of biodegradation alteration. Moreover, parameters MCI1 [MCI1 = 1.5 (2-MChy + 3-MChy)/(chrysene + 1-MChy + 4-MChy + 5-MChy + 6-MChy),[5] MCI2 [MCI2 = (2-MChy + 3-MChy)/(1-MChy + 4-MChy + 5-MChy + 6-MChy),[5] and MChyI2 (MChyI2 = 3-MChy/1-MChy[59]) show an obvious positive correlation with increasing biodegradation while parameter C_{28} TAS remains constant (Figure 11a–d).[39] This also suggests that these three maturity parameters increase with increasing biodegradation degree, while parameter C_{28} TAS is still valid in PM 8. Maturity parameters MDR (MDR = 4-methylDBT/1-methylDBT[2]) and

https://doi.org/10.1021/acsearthspacechem.2c00378
ACS Earth Space Chem. 2023, 7, 823−837

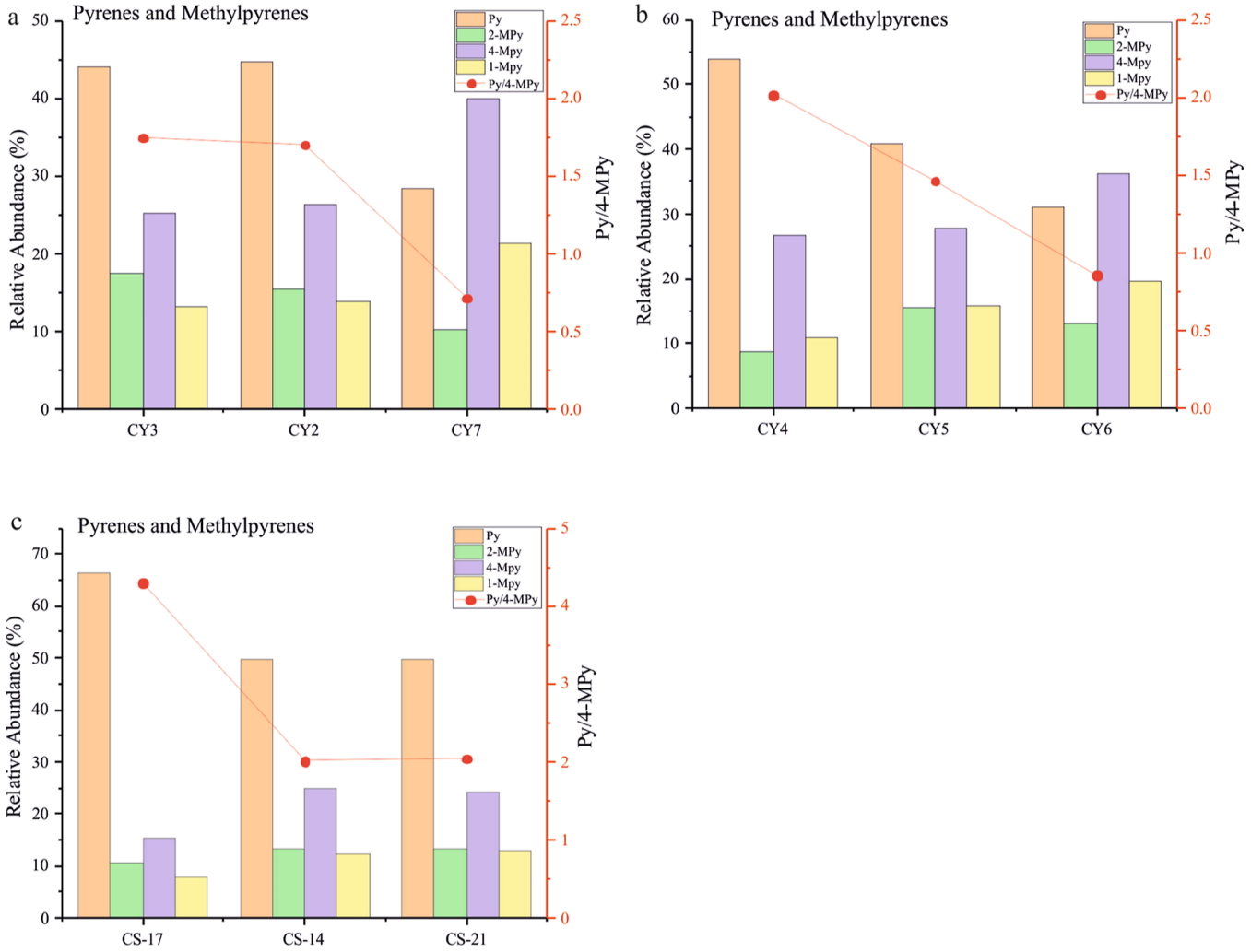

Figure 9. Bar graphs showing the relative abundance (%) of components in crude oils (a,b) and oil sands (c) from the Chepaizi Uplift, Junggar Basin with increasing biodegradation: pyrene (Py) and methylpyrenes (MPy).

DMDBTI [DMDBTI = (4,6-+2,4-DMDBT)/(1,4-+1,6+1,8-+4,6-+2,4-DMDBT)[3] show a negative correlation with increasing biodegradation (Figure 11e). These two parameters decrease with increasing biodegradation. In addition, from these cross-plots (Figure 11), we can also conclude that sample CY6 is the most biodegraded. However, maturity parameters such as PP-1, MPI-1, MpyI1, and MpyI2 were irregularly changed due to biodegradations (Table 3, Figure 11f–h). Therefore, we should be cautious when using PAH-based maturity parameters, and the relative susceptibilities of individual PAH components to biodegradation should be taken into consideration, especially in areas where oils are severely degraded.

As mentioned above, C_{20} TAS and C_{21} TAS start to be removed before C_{26}–C_{28} TAS, as the relative abundance of C_{26}–C_{28} TAS does not exhibit any variations even at PM 8. Therefore, C_{26}–C_{28} TAS remains a valid indicator for oil–oil correlations when regular steranes and hopanes have been severely attacked or attacked to complete removal. We have determined the relative abundance of C_{26}, C_{27}, and C_{28} TAS on the basis of the method proposed by Baoshou.[61] The results show that these oil samples are derived from the same source bed/kitchen and can be considered to be derived from the same oil family (Figure 12a). However, in the ternary diagram of the relative abundance of fluorene, dibenzothiophene, and dibenzofuran for oil–source/oil–oil correlations, the samples show a dispersed distribution except for the slightly biodegraded oil sand group (oil sand samples CS-17, CS-14, CS-21), which can affect our conclusions (Figure 12b).

5. CONCLUSIONS

GC–MS analyses of oils and oil sands from the Chepaizi Uplift, Junggar Basin reveal that biodegradation has a significant effect on the composition of PAHs. The relative susceptibilities of the individual dibenzothiophene, fluorene, chrysene, and pyrene and their alkylated homologues, and triaromatic steroid hydrocarbons were determined in Table 2. Different from the common understanding, fluorene without methyl is more resistant to biodegradation than 1-MF. Moreover, maturity assessment parameters, including DBT/1-MDBT, 3,7-/2,4-DMDBT, 1,2,7-+1,2,8-/2,4,6-TMDBT, 1-MF/4-MF, Ch/3-MCh, and Py/4-MPy, are proposed in terms of the relative changes in isomeric distribution during increasing biodegradation. The process of biodegradation is widespread in oils, and determining its level usually appears to be more complex, especially for severe biodegradation.

The relative susceptibilities of PAHs are mainly dependent upon the position of alkylation or the degree of alkylation

https://doi.org/10.1021/acsearthspacechem.2c00378
ACS Earth Space Chem. 2023, 7, 823–837

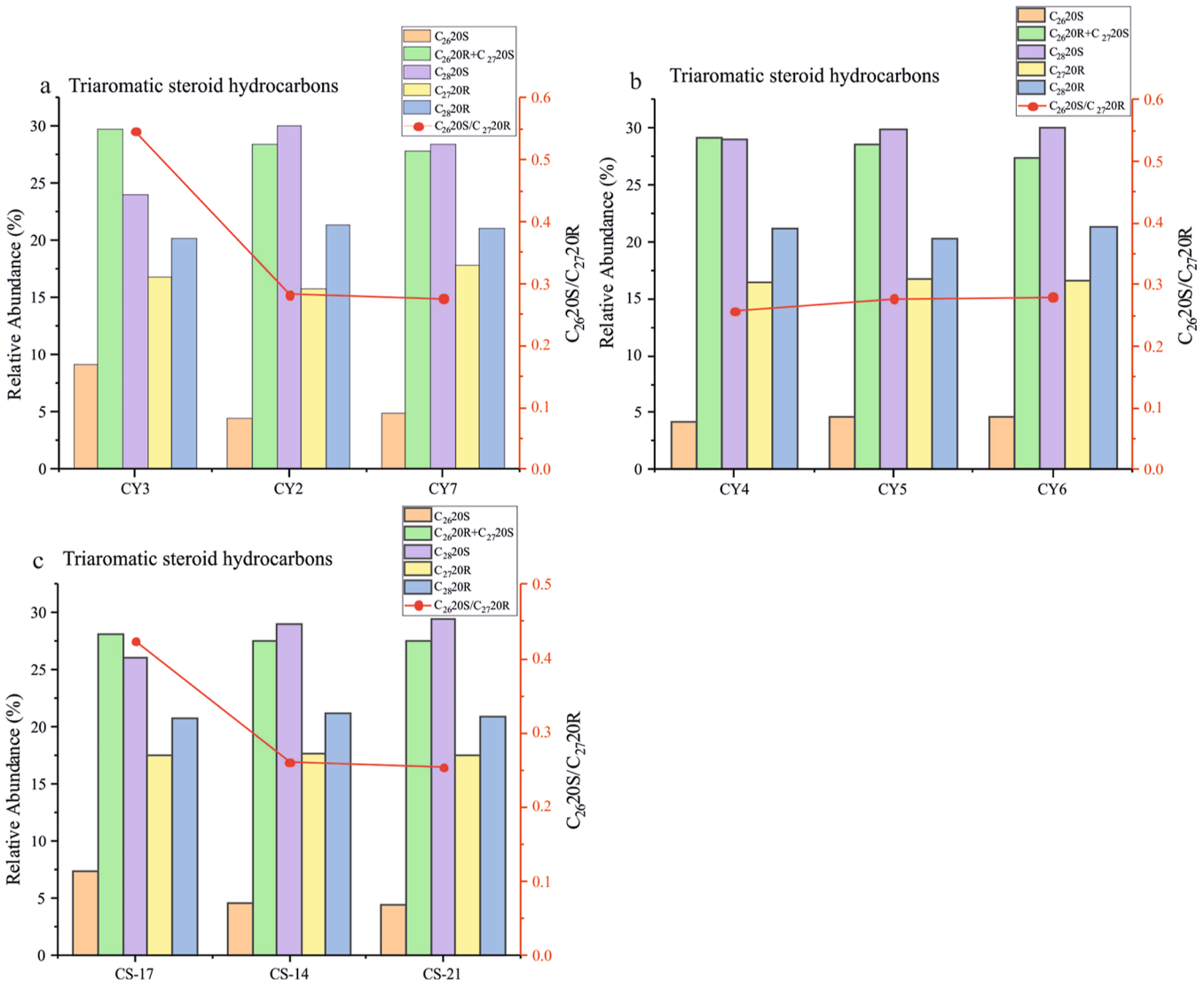

Figure 10. Bar graphs showing the relative abundance (%) of C_{26}−C_{28} triaromatic steroids in crude oils (a,b) and oil sands (c) from the Chepaizi Uplift, Junggar Basin with increasing biodegradation.

Table 2. Summary of the Order of Resistance of PAHs to Biodegradation in Crude Oils and Oil Sands from the Chepaizi Area, Junggar Basin

compounds	most susceptible, least susceptible	biodegradation parameters
dibenzothiophenes	DBT, MDBT: DBT > 2-+3- > 4- ≫ 1-	DBT/1-MDBT
	DMDBT: 3,7- > 2,4- ∼ 2,6- > 1,3-+1,9- > 1,4-+1,6-+1,8- > 3,6- > 1,2- > 4-ethyl- > 4,6-	3,7-/2,4-DMDBT
	TMDBT: 1,2,7-+1,2,8- > 1,3,7- > 4-ethyl-6- > 1,2,4- > 1,4,6- > 1,4,8- > 3,4,6- > 2,4,6-	1,2,7-+1,2,8-/2,4,6-TMDBT
fluorenes	F and MF: 1-MF > F > 2-MF > 3-MF > 4-MF	1-MF/4-MF
	DMF: 1,6-DMF > 1,8-DMF > 1,3-DMF > 1,7-DMF ∼ A > B (oils)	1,6-DMF/B
	DMF: 1,7-DMF > B > 1,8-DMF > A ∼ 1,3-DMF > 1,6-DMF (oil sands)	1,6-DMF/B
chrysenes	Ch and MCh: 2- ∼ 1- > 4-+6- > Ch ≫ 3-	Ch/3-MCh[33]
pyrenes	Py and Mpy: Py > 2- > 4- > 1-	Py/4-MPy
triaromatic steroid hydrocarbons	C_{20}−C_{21} TAS > C_{26}−C_{28} TAS	C_{26}20S TAS/C_{27}20R TAS
	C_{26}20S TAS > C_{26}20R+C_{27}20S TAS > C_{27}20R TAS ∼ C_{28}20R TAS > C_{28}20S TAS	

(rather than their thermodynamic stability), making maturity assessment more complex. The reliable PAH maturity parameter is the C_{28} triaromatic steroid ratio 20S/(20S + 20R) before PM 9. Except for C_{28} TAS, the PAH-based maturity parameters increased or decreased to varying degrees, which are not reliable for maturity assessment. Maturity parameters, such as MCI1, MCI2, and MChyI2, increase with increasing biodegradation, while MDR and DMDBTI decrease with increasing biodegradation. However, maturity parameters, such as PP-1, MPI-1, MpyI1, and MpyI2 were irregularly changed due to biodegradation. C_{26}−C_{28} TAS remains a valid indicator for oil−oil correlations when regular steranes and hopanes have been severely attacked or attacked to complete removal, while the other biomarker indicators, such as the

https://doi.org/10.1021/acsearthspacechem.2c00378
ACS Earth Space Chem. 2023, 7, 823−837

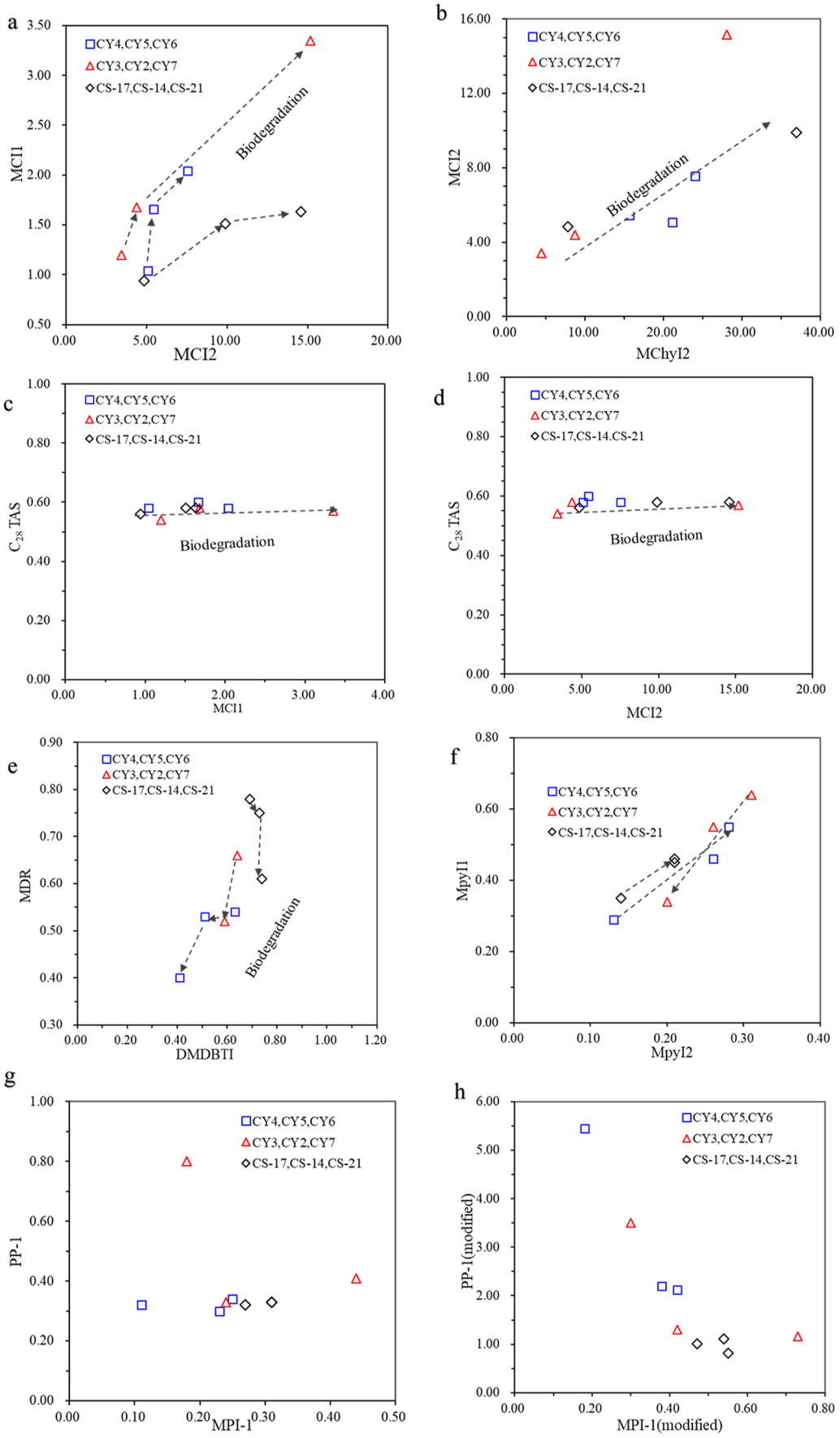

Figure 11. Cross-plots of maturity parameters in the Carboniferous oils and oil sands from the Chepaizi area, Junggar Basin.

https://doi.org/10.1021/acsearthspacechem.2c00378
ACS Earth Space Chem. 2023, 7, 823−837

Table 3. PAH Maturity Parameters of the Representative Crude Oil and Oil Sand Samples[a]

PAH maturity parameters	CY4	CY5	CY6	CY3	CY2	CY7	CS-17	CS-14	CS-21
PP-1	0.32	0.34	0.30	0.41	0.80	0.33	0.33	0.33	0.32
$PP\text{-}1_{(modified)}$	5.45	2.12	2.20	1.16	3.50	1.30	0.81	1.11	1.01
MPI-1	0.11	0.25	0.23	0.44	0.18	0.24	0.31	0.31	0.27
$MPI\text{-}1_{(modified)}$	0.18	0.42	0.38	0.73	0.30	0.42	0.55	0.54	0.47
MDR	0.54	0.53	0.40	0.66	0.52		0.78	0.75	0.61
DMDBTI	0.63	0.51	0.41	0.64	0.59		0.69	0.73	0.74
TMDBTI				3.75	4.69	5.07	7.16		
MCI1	1.04	1.66	2.04	1.20	1.68	3.35	0.94	1.51	1.63
MCI2	5.08	5.44	7.55	3.42	4.39	15.17	4.84	9.90	14.56
MChyI1	1.76	1.16	0.29	0.90	0.95	1.43	1.69	2.16	
MChyI2	21.14	15.66	24.00	4.44	8.76	28.03	7.87	36.89	
MpyI1	0.29	0.55	0.46	0.64	0.55	0.34	0.35	0.46	0.45
MpyI2	0.13	0.28	0.26	0.31	0.26	0.20	0.14	0.21	0.21
TAS	0.08	0.08	0.05	0.08	0.14	0.14	0.08	0.21	0.09
C_{28} TAS	0.56	0.60	0.56	0.54	0.56	0.57	0.56	0.56	0.56

[a]Abbreviations: PP-1 = 1MPe/(2MPe + 3MPe),[60] $PP\text{-}1_{(modified)}$ = (1MPe + 9MPe)/(2MPe + 3MPe),[39] MPI-1 = (2MPe + 3MPe)/(Phe + 1MPe + 9MPe),[8] $MPI\text{-}1_{(modified)}$ = 1.89 × (2MPe + 3MPe)/(Phe + 1.26 × (1MPe + 9MPe)),[39] MDR = 4-methylDBT/1-methylDBT,[2] DMDBTI = (4,6-+2,4-DMDBT)/(1,4-+1,6+1,8-+4,6-+2,4-DMDBT),[3] TMDBTI = 2,4,6-TMDBT/(2,4,7-+2,4,8-TMDBT),[4] MCI1 = 1.5 (2-MChy + 3-MChy)/(chrysene + 1-MChy + 4-MChy + 5-MChy + 6-MChy),[5] MCI2 = (2-MChy + 3-MChy)/(1-MChy + 4-MChy + 5-MChy + 6-MChy),[5] MChyI1 = 2-MChy/1-MChy,[10] MChyI2 = 3-MChy/1-MChy,[59] MpyI1 = 3 × 2-MPY/(1-+4-+MPY),[5] MpyI2 = 2-MPY/(1-+2-MPY)[5] TAS = (C_{20} + C_{21} triaromatic steroids)/(C_{20} + C_{21} + C_{26} + C_{27} + C_{28} triaromatic steroids),[6] C_{28} TAS = C_{28} triaromatic steroid 20S/(20S + 20R).[7]

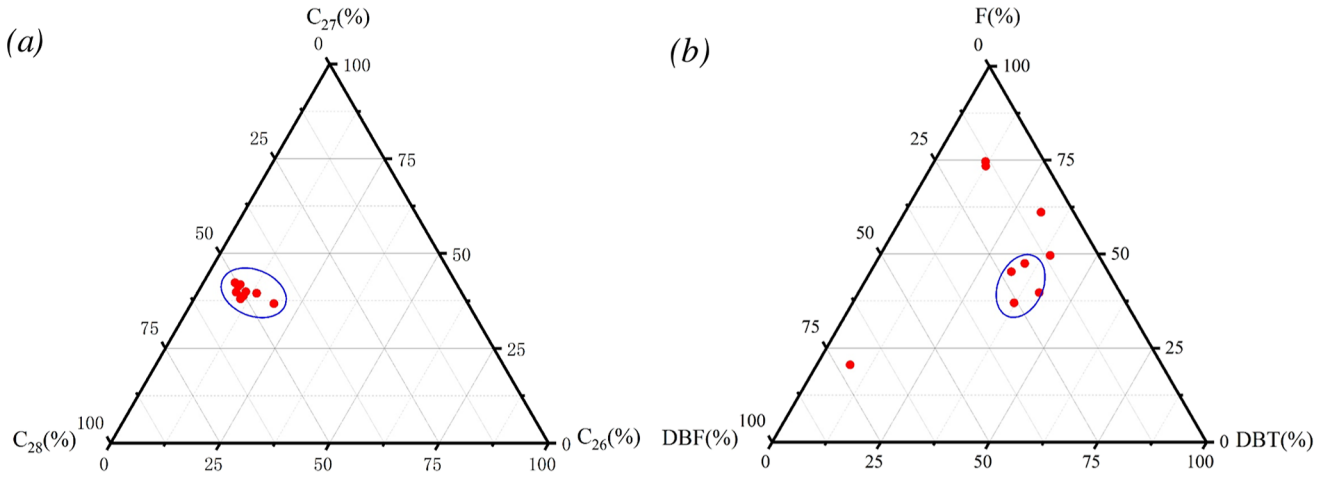

Figure 12. (a) Ternary diagram of the relative abundance of triaromatic steroids classifying oil families of the Carboniferous reservoir in the Chepaizi Uplift, Junggar Basin, NW China. (b) Ternary diagram of the relative abundance of DBT, DBF, and F classifying oil families of the Carboniferous reservoir in the Chepaizi Uplift, Junggar Basin, NW China.

relative abundance of fluorene, dibenzothiophene, and dibenzofuran, are no longer reliable.

■ ASSOCIATED CONTENT

Supporting Information

The Supporting Information is available free of charge at https://pubs.acs.org/doi/10.1021/acsearthspacechem.2c00378.

Partial mass chromatograms (m/z 231), (m/z 184 + 198 + 212), (m/z 166 + 180 + 194), (m/z 228 + 242), (m/z 202 + 216), and (m/z 191 and m/z 177) showing the distributions of triaromatic steroid hydrocarbons; dibenzothiophene, methyldibenzothiophenes, and C_2-dibenzothiophenes; fluorene, methylfluorenes, and C_2-fluorenes; chrysene and methylchrysenes; pyrene and methylpyrenes; and C_{29} 17α(H),21β(H) 25-norhopane, demethylated tricyclic terpanes, and tricyclic terpanes in aromatic fractions of representative crude oils and oil sand with increasing extent of biodegradation from the Chepaizi Uplift (PDF)

■ AUTHOR INFORMATION

Corresponding Author

Zhihuan Zhang − *State Key Laboratory of Petroleum Resources and Prospecting, China University of Petroleum (Beijing), Beijing 102249, China; College of Geoscience, China University of Petroleum, Beijing 102249, China;* orcid.org/0000-0001-9224-3365; Email: zhangzh3996@vip.163.com

Authors

Xue Chen − *State Key Laboratory of Petroleum Resources and Prospecting, China University of Petroleum (Beijing), Beijing 102249, China; College of Geoscience, China University of Petroleum, Beijing 102249, China*

Ningrui Yang − *State Key Laboratory of Petroleum Resources and Prospecting, China University of Petroleum (Beijing),*

https://doi.org/10.1021/acsearthspacechem.2c00378
ACS Earth Space Chem. 2023, 7, 823−837

Beijing 102249, China; College of Geoscience, China University of Petroleum, Beijing 102249, China

Xiao Jin − *Development and Research Center, National Geological Archives of China, China Geological Survey, Beijing 100037, China*

Ruihui Zheng − *State Key Laboratory of Petroleum Resources and Prospecting, China University of Petroleum (Beijing), Beijing 102249, China; College of Geoscience, China University of Petroleum, Beijing 102249, China*

Yunpeng Zhang − *Shengli Oilfield Branch, SINOPEC, Dongying, Shandong 257000, China*

Complete contact information is available at: https://pubs.acs.org/10.1021/acsearthspacechem.2c00378

Notes

The authors declare no competing financial interest.

■ ACKNOWLEDGMENTS

We would like to thank the reviewers for their helpful comments, suggestions, and scientific and linguistic revisions of the manuscript. We are grateful to SINOPEC Shengli Oilfield (China) for supplying the samples and providing original geological data. In addition, we thank the State Key Laboratory of Petroleum Resources and Prospecting for GC−MS analysis.

■ ABBREVIATIONS

PAHs, polycyclic aromatic hydrocarbons; PM, Peters and Moldowan scale; 9-MP, 9-methylphenanthrene; 1,7-DMP, 1,7-dimethylphenanthrene; GC−MS, gas chromatography−mass spectrometry; SIM, selective ion monitoring; TIC, total ion current; TICs, total ion chromatograms; UCM, unresolved complex mixture; C_{30}H, C_{30} 17α(H) hopane; TTs, tricyclic terpanes; NTT, demethylated tricyclic terpanes; Preg, C_{21}−C_{22} steranes; C_{28} TAS, C_{28} triaromatic steroid 20S/(20S + 20R); D_{29}, C_{29} 25-norhopane; G, gammacerane; St, steranes; C_{24}TeT, C_{24} tetracyclic terpane; Ts, 18α-trisnorneohopane; Tm, 17α-trisnorhopane; 29Dia, C_{29} diasteranes; P, phenanthrene; EP, 3-ethylphenanthrene; DBT, dibenzothiophene; MDBT, methyldibenzothiophene; DMDBT, dimethyldibenzothiophene; EDBT, ethyldibenzothiophene; TMDBT, trimethyldibenzothiophene; 4-E-6-M, 4-ethyl-6-methyldibenzothiophene; F, fluorenes; MF, methylfluorene; Ch, chrysene; MCh, methlchrysenes; Py, pyrene; MPy, methylpyrenes; TAS, triaromatic steroid

■ REFERENCES

(1) Tissot, B. P.; Welte, D. H. *Petroleum Formation and Occurrence*; Springer-Verlag: Berlin, 1978.

(2) Radke, M.; Welte, D. H.; Willsch, H. Maturity parameters based on aromatic hydrocarbons: Influence of the organic matter type. *Org. Geochem.* **1986**, *10*, 51−63.

(3) Kruge, M. A. Determination of thermal maturity and organic matter type by principal components analysis of the distributions of polycyclic aromatic compounds. *Int. J. Coal Geol.* **2000**, *43*, 27−51.

(4) Li, M.; Zhong, N.; Shi, S.; Zhu, L.; Tang, Y. The origin of trimethyldibenzothiophenes and their application as maturity indicators in sediments from the Liaohe Basin, East China. *Fuel* **2013**, *103*, 299−307.

(5) Garrigues, P.; De Sury, R.; Angelin, M. L.; Bellocq, J.; Oudin, J. L.; Ewald, M. Relation of the methylated aromatic hydrocarbon distribution pattern to the maturity of organic matter in ancient sediments from the Mahakam delta. *Geochim. Cosmochim. Acta* **1988**, *52*, 375−384.

(6) Mackenzie, A. S.; Hoffmann, C. F.; Maxwell, J. R. Molecular parameters of maturation in the Toarcian shales, Paris Basin, France—III. Changes in aromatic steroid hydrocarbons. *Geochim. Cosmochim. Acta* **1981**, *45*, 1345−1355.

(7) Peters, K. E.; Moldowan, J. M. *The Biomarker Guide*, 2nd ed.; Cambridge University Press: Cambridge, UK, 2005.

(8) Radke, M.; Welte, D. H.; Willsch, H. Geochemical study on a well in the Western Canada Basin: relation of the aromatic distribution pattern to maturity of organic matter. *Geochim. Cosmochim. Acta* **1982**, *46*, 1−10.

(9) Chakhmakhchev, A.; Suzuki, M.; Takayama, K. Distribution of alkylated dibenzothiophenes in petroleum as a tool for maturity assessments. *Org. Geochem.* **1997**, *26*, 483−489.

(10) Li, M.; Shi, S.; Wang, T. G. Identification and distribution of chrysene, methylchrysenes and their isomers in crude oils and rock extracts. *Org. Geochem.* **2012**, *52*, 55−66.

(11) Xu, H.; George, S. C.; Hou, D. Algal-derived polycyclic aromatic hydrocarbons in Paleogene lacustrine sediments from the Dongying Depression, Bohai Bay Basin, China. *Mar. Pet. Geol.* **2019**, *102*, 402−425.

(12) Pu, F.; Philip, R. P.; Zhenxi, L.; Guangguo, Y. Geochemical characteristics of aromatic hydrocarbons of crude oils and source rocks from different sedimentary environments. *Org. Geochem.* **1990**, *16*, 427−435.

(13) Picha, F. J. A.; Peters, K. E. B. Biomarker oil-to-source rock correlation in the Western Carpathians and their foreland, Czech Republic. *Pet. Geosci.* **1998**, *4*, 289−302.

(14) Wang, T.; He, F.; Li, M.; Hou, Y.; Guo, S. Alkyldibenzothiophenes: molecular tracers for filling pathway in oil reservoirs. *Chin. Sci. Bull.* **2004**, *49*, 2399−2404.

(15) Sivan, P.; Datta, G. C.; Singh, R. R. Aromatic biomarkers as indicators of source, depositional environment, maturity and secondary migration in the oils of Cambay Basin, India. *Org. Geochem.* **2008**, *39*, 1620−1630.

(16) Bao, J.; Zhu, C. The effects of biodegradation on the compositions of aromatic hydrocarbons and maturity indicators in biodegraded oils from Liaohe Basin. *Sci. China, Ser. D: Earth Sci.* **2009**, *52*, 59−68.

(17) Hossain, H. M. Z.; Sampei, Y.; Roser, B. P. Polycyclic aromatic hydrocarbons (PAHs) in late Eocene to early Pleistocene mudstones of the Sylhet succession, NE Bengal Basin, Bangladesh: Implications for source and paleoclimate conditions during Himalayan uplift. *Org. Geochem.* **2013**, *56*, 25−39.

(18) Li, M.; Simoneit, B. R. T.; Zhong, N.; Fang, R. The distribution and origin of dimethyldibenzothiophenes in sediment extracts from the Liaohe Basin, East China. *Org. Geochem.* **2013**, *65*, 63−73.

(19) Fang, R.; Li, M.; Wang, T. G.; Liu, X.; Yuan, Y.; Jiang, W.; Wang, D.; Shi, S. Trimethyldibenzothiophenes: Molecular tracers for filling pathways in oil reservoir. *J. Pet. Sci. Eng.* **2017**, *159*, 451−460.

(20) Volkman, J. K.; Alexander, R.; Kagi, R. I.; Rowland, S. J.; Sheppard, P. N. Biodegradation of aromatic hydrocarbons in crude oils from the Barrow Sub-basin of Western Australia. *Org. Geochem.* **1984**, *6*, 619−632.

(21) Williams, J. A.; Bjorøy, M.; Dolcater, D. L.; Winters, J. C. Biodegradation in south Texas Eocene oils-effects on aromatics and biomarkers. *Org. Geochem.* **1986**, *10*, 451−461.

(22) Fisher, S. J.; Alexander, R.; Kagi, R. I. Biodegradation of alkylnaphthalenes in sediments adjacent to an offshore petroleum production platform. *Polycyclic Aromat. Compd.* **1996**, *11*, 35−42.

(23) Huang, H.; Bowler, B. F. J.; Oldenburg, T. B. P.; Larter, S. R. The effect of biodegradation on polycyclic aromatic hydrocarbons in reservoired oils from the Liaohe basin, NE China. *Org. Geochem.* **2004**, *35*, 1619−1634.

(24) George, S. C.; Boreham, C. J.; Minifie, S. A.; Teerman, S. C. The effect of minor to moderate biodegradation on C_5 to C_9 hydrocarbons in crude oils. *Org. Geochem.* **2002**, *33*, 1293−1317.

(25) Cheng, X.; Hou, D.; Xu, C.; Wang, F. Biodegradation of tricyclic terpanes in crude oils from the Bohai Bay Basin. *Org. Geochem.* **2016**, *101*, 11−21.

(26) Sabaté, J.; Grifoll, M.; Viñas, M.; Solanas, A. M. Isolation and characterization of a 2-methylphenanthrene utilizing bacterium: identification of ring cleavage metabolites. *Appl. Microbiol. Biotechnol.* **1999**, *52*, 704−712.
(27) Vila, J.; López, Z.; Sabaté, J.; Minguillón, C.; Solanas, A. M.; Grifoll, M. Identification of a novel metabolite in the degradation of pyrene by Mycobacterium sp strain AP1: Actions of the isolate on two- and three-ring polycyclic aromatic hydrocarbons. *Appl. Environ. Microbiol.* **2001**, *67*, 5497−5505.
(28) Dean-Ross, D.; Moody, J.; Cerniglia, C. E. Utilization of mixtures of polycyclic aromatic hydrocarbons by bacteria isolated from contaminated sediment. *FEMS Microbiol. Ecol.* **2002**, *41*, 1−7.
(29) Peters, K. E.; Moldowan, J. M. *The Biomarker Guide: Interpreting Molecular Fossils in Petroleum and Ancient Sediments*; Prentice Hall: Englewood Cliffs NJ, 1993.
(30) Wenger, L. M.; Davis, C. L.; Isaksen, G. H. Multiple controls on petroleum biodegradation and impact on oil quality. *SPE Reservoir Eval. Eng.* **2002**, *5*, 375−383.
(31) Larter, S. R.; Huang, H.; Adams, J.; Bennett, B.; Snowdon, L. R. A practical biodegradation scale for use in reservoir geochemical studies of biodegraded oils. *Org. Geochem.* **2012**, *45*, 66−76.
(32) Wang, X.; Cai, T.; Wen, W.; Ai, J.; Ai, J.; Zhang, Z.; Zhu, L.; George, S. C. Surfactin for enhanced removal of aromatic hydrocarbons during biodegradation of crude oil. *Fuel* **2020**, *267*, 117272.
(33) Huang, H.; Yin, M.; Han, D. Novel parameters derived from alkylchrysenes to differentiate severe biodegradation influence on molecular compositions in crude oils. *Fuel* **2020**, *268*, 117366.
(34) Chen, J.; Zhang, H.; Huang, H.; Li, X.; Shi, S.; Liu, F.; Chen, L. Impact of anaerobic biodegradation on alkylphenanthrenes in crude oil. *Org. Geochem.* **2013**, *61*, 6−14.
(35) Bennett, B.; Larter, S. R. Biodegradation scales: Application and limitations. *Org. Geochem.* **2008**, *39*, 1222−1228.
(36) Connan, J. Biodegradation of crude oils in reservoirs. In *Advances in Petroleum Geochemistry*; Brooks, J., Welte, D., Eds.; Academic Press: London, 1984; pp 299−335.
(37) Palmer, S. E. Effect of biodegradation and water washing on crude oil composition. *Top. Geobiol.* **1993**, *11*, 511−533.
(38) Rowland, S. J.; Alexander, R.; Kagi, R. I.; Jones, D. M. Microbial degradation of aromatic components of crude oils: A comparison of laboratory and field observations. *Org. Geochem.* **1986**, *9*, 153−161.
(39) Cassani, F.; Eglinton, G. Organic geochemistry of Venezuelan extra-heavy crude oils 2. Molecular assessment of biodegradation. *Chem. Geol.* **1991**, *91*, 315−333.
(40) Budzinski, H.; Raymond, N.; Nadalig, T.; Gilewicz, M.; Garrigues, P.; Bertrand, J. C.; Caumette, P. Aerobic biodegradation of alkylated aromatic hydrocarbons by a bacterial community. *Org. Geochem.* **1998**, *28*, 337−348.
(41) Weifeng, W.; Yequan, C. Tectonic evolution and petroleum systems in the Junggar Basin. *Acta Geol. Sin.* **2010**, *78*, 667−675.
(42) Chang, X.; Zhao, H.; He, W.; Xu, Y.; Xu, Y.; Wang, Y. Improved understanding of the alteration of molecular compositions by severe to extreme biodegradation: a case study from the Carboniferous oils in the eastern Chepaizi Uplift, Junggar Basin, northwest China. *Energy Fuels* **2018**, *32*, 7557−7568.
(43) Shi, B.; Chang, X.; Xu, Y.; Wang, Y.; Mao, L.; Wang, Y. Origin and migration pathway of biodegraded oils pooled in multiple-reservoirs of the Chepaizi Uplift, Junggar Basin, NW China: Insights from geochemical characterization and chemometrics methods. *Mar. Pet. Geol.* **2020**, *122*, 104655.
(44) Cao, J.; Jin, Z.; Hu, W.; Zhang, Y.; Yao, S.; Wang, X.; Zhang, Y.; Tang, Y. Improved understanding of petroleum migration history in the Hongche fault zone, northwestern Junggar Basin (northwest China): Constrained by vein-calcite fluid inclusions and trace elements. *Mar. Pet. Geol.* **2010**, *27*, 61−68.
(45) Xiang, B.; Zhou, N.; Ma, W.; Wu, M.; Cao, J. Multiple-stage migration and accumulation of Permian lacustrine mixed oils in the central Junggar Basin (NW China). *Mar. Pet. Geol.* **2015**, *59*, 187−201.
(46) Xu, Y.; Chang, X.; Shi, B.; Wang, Y.; Li, Y. Geochemistry of severely biodegraded oils in the Carboniferous volcanic reservoir of the Chepaizi Uplift, Junggar Basin, NW China. *Energy Explor. Exploit.* **2018**, *36*, 1461−1481.
(47) Peters, K. E.; Moldowan, J. M.; McCaffrey, M. A.; Fago, F. J. Selective biodegradation of extended hopanes to 25-norhopanes in petroleum reservoirs. Insights from molecular mechanics. *Org. Geochem.* **1996**, *24*, 765−783.
(48) Goodwin, N. S.; Park, P. J. D.; Rawlinson, A. P. Crude oil biodegradation under simulated and natural conditions. In *Advances in Organic Geochemistry*; Bjorøy, M., Albrecht, P., Cornford, C., de Groot, K., Eglinton, G., Galimov, E., Leythaeuser, D., Pelet, R., Rullkötter, J., Speers, G., Eds.; John Wiley & Sons: Chichester, 1981; pp 650−658.
(49) Bost, F. D.; Frontera-Suau, R.; McDonald, T. J.; Peters, K. E.; Morris, P. J. Aerobic biodegradation of hopanes and norhopanes in Venezuelan crude oils. *Org. Geochem.* **2001**, *32*, 105−114.
(50) Alberdi, M.; Moldowan, J. M.; Peters, K. E.; Dahl, J. E. Stereoselective biodegradation of tricyclic terpanes in heavy oils from the Bolivar Coastal Fields, Venezuela. *Org. Geochem.* **2001**, *32*, 181−191.
(51) Spigolon, A. L. D.; Cerqueira, J. R.; Binotto, R.; Fontes, R. A.; Silva, T. F.; Bautista, D. F. G. Source rock characteristics predicted based on MSSV pyrolysis of asphaltenes from a severely biodegraded oil. *Rev. Latinoam. Geoquim. Org.* **2010**, *1*, 14−24.
(52) Garcia Bautista, D. F.; Vaz dos Santos Neto, E.; Penteado, H. L. B. Controls on petroleum composition in the Llanos Basin, Colombia: implications for exploration. *AAPG Bull.* **2015**, *99*, 1503−1535.
(53) Volkman, J. K.; Alexander, R.; Kagi, R. I.; Woodhouse, G. W. Demethylated hopanes in crude oils and their applications in petroleum geochemistry. *Geochim. Cosmochim. Acta* **1983**, *47*, 785−794.
(54) Larter, S.; Wilhelms, A.; Head, I.; Koopmans, M.; Aplin, A.; Di Primio, R.; Zwach, C.; Erdmann, M.; Telnaes, N. The controls on the composition of biodegraded oils in the deep subsurface—part 1: biodegradation rates in petroleum reservoirs. *Org. Geochem.* **2003**, *34*, 601−613.
(55) Zhi-huan, Z.; Hong-jun, L.; Wei, L.; Jia-jia, F.; Kui, X.; Li-ming, Q.; Wei-jun, X.; Lei, Z. Origin and accumulation process of heavy oil in Chepaizi area of Junggar Basin. *J. Earth Sci. Environ.* **2014**, *36*, 18−32. (in Chinese)
(56) Mazeas, L.; Budzinski, H.; Raymond, N. Absence of stable carbon isotope fractionation of saturated and polycyclic aromatic hydrocarbons during aerobic bacterial biodegradation. *Org. Geochem.* **2002**, *33*, 1259−1272.
(57) Asif, M.; Alexander, R.; Fazeelat, T.; Grice, K. Sedimentary processes for the geosynthesis of heterocyclic aromatic hydrocarbons and fluorenes by surface reactions. *Org. Geochem.* **2010**, *41*, 522−530.
(58) Wardroper, A. M. K.; Hoffmann, C. F.; Maxwell, J. R.; Barwise, A. J. G.; Goodwin, N. S.; Park, P. J. D. Crude oil biodegradation under simulated and natural conditions—II. Aromatic steroid hydrocarbons. *Org. Geochem.* **1984**, *6*, 605−617.
(59) Shen, Z.; Wei, J.; Zhu, H.; Liu, S.; Dang, H. Comparative research on maturity feature and maturity indicator of coal source rock from west Sichuan Basin Depression. *Mineral. Petrol.* **2009**, *29*, 83−88.
(60) Alexander, R.; Strachan, M.; Kagi, R.; Van Bronswijk, W. Heating rate effects on aromatic maturity indicators. *Org. Geochem.* **1986**, *10*, 997−1003.
(61) Baoshou, Z.; Meijun, L.; Qing, Z.; Tieguan, W.; Ke, Z.; Zhongyao, X.; Shaoying, H. Determining the relative abundance of C_{26}-C_{28} triaromatic steroids in crude oils and its application in petroleum geochemistry. *Pet. Geol. Exp.* **2016**, *38*, 692−697. (in Chinese)

https://doi.org/10.1021/acsearthspacechem.2c00378
ACS Earth Space Chem. 2023, 7, 823−837